



Divergent responses of soil microorganisms to throughfall exclusion across tropical forest soils driven by soil fertility and climate history



Stephany S. Chacon^{a,*}, Daniela F. Cusack^{b,c}, Aizah Khurram^a, Markus Bill^a, Lee H. Dietterich^b, Nicholas J. Bouskill^{a,**}

^a Climate and Ecosystem Sciences Division, Lawrence Berkeley National Laboratory, Berkeley, CA, 94720, USA

^b Department of Ecosystem Science and Sustainability, Colorado State University, Fort Collins, CO, 80523, USA

^c Smithsonian Tropical Research Institute, Apartado, 0843-03092, Balboa, Ancon, Panama

ARTICLE INFO

Keywords:

Field
Throughfall exclusion
Microbial community
Tropical rainforest
Panama
SOM
Mean annual precipitation
Soil fertility

ABSTRACT

Model projections predict tropical forests will experience longer periods of drought and more intense precipitation cycles under a changing climate. Such transitions have implications for structure-function relationships within microbial communities. We examine how throughfall exclusion might reshape prokaryotic and fungal communities across four lowland forests in Panama with a wide variation in mean annual precipitation and soil fertility. Four sites were established across a 1000 mm span in Mean Annual Precipitation (MAP: 2335–3421 mm). We expected microbial communities at sites with lower MAP to be less sensitive to throughfall exclusion than sites with higher MAP and fungal communities to be more resistant to disturbance than prokaryotes. At each location, partial throughfall exclusion structures were established over 10 × 10 m plots to reduce direct precipitation input. After short-term (~3–9 months) throughfall exclusion, prokaryotic communities showed no change in composition. However, prolonged (12–18 months) throughfall exclusion resulted in divergent prokaryotic community responses, reflecting MAP and soil fertility. We observed the emergence of a “drought microbiome” within infertile sites, whereby the community structure of the experimental throughfall exclusion plots at the lower MAP sites diverged from their respective control sites and converged towards overlapping assemblages. Furthermore, under throughfall exclusion, taxa increasing in relative abundance at the wettest site reflected that endemic to control plots at the lowest MAP site, suggesting a shift toward communities with life-history traits selected for under a lower MAP. By contrast, fungal community composition across sites was resilient to throughfall exclusion; however, biomass diverged in response to throughfall exclusion, increasing at two sites while decreasing in the other two. Broadly, our results suggest that microbial communities’ sensitivity to frequent drying and rewetting periods in tropical forest soils will depend on climate history and soil fertility, with infertile sites likely to respond readily to changes in precipitation.

1. Introduction

Tropical forest soils contain some of the largest carbon stocks on Earth (Crowther et al., 2019; Jackson et al., 2017). Humid and warm conditions promote high primary productivity, which offsets high ecosystem respiration rates (Bonan, 2008; Malhi and Grace, 2000). This balance in productivity and respiration has resulted in significant carbon accumulation in plant biomass and soils within tropical forests. These vast carbon stocks can be destabilized under a changing climate (Mitchard, 2018; Sullivan et al., 2020), and model projections predict

tropical and subtropical regions will experience disturbance to the hydrological cycle, with an increased likelihood of more frequent and prolonged droughts interspersed with periods of intense precipitation (Chadwick et al., 2016; Easterling et al., 2000; Meehl et al., 2006). Drought within tropical regions has previously been demonstrated to disrupt soil nutrient cycling (O’Connell et al., 2018) and may decrease tropical forest C storage (Cusack et al., 2011; Doughty et al., 2014; Gatti et al., 2014; Phillips et al., 2009).

The impact of soil drying on microbial communities within tropical forest soils remains poorly understood. The resistance and resilience of a

* Corresponding author.

** Corresponding author.

E-mail addresses: sschacon@lbl.gov (S.S. Chacon), njbouskill@lbl.gov (N.J. Bouskill).

community are mainly shaped by historical contingencies (Evans and Wallenstein, 2014; Hawkes and Keitt, 2015). Thus, past and present climate, in particular, mean annual precipitation (MAP) and dry season lengths, are likely important in determining the sensitivity of soil microbes to drought (Azarbad et al., 2020). Therefore, regions with high precipitation may be more sensitive to seldomly experienced environmental changes, such as soil drying (Bouskill et al., 2013; Hawkes and Keitt, 2015). Indeed, microbial communities without a historical legacy of drought have exhibited profound shifts in community composition (Bouskill et al., 2013), function (Bouskill et al., 2016a; Bouskill et al., 2016b; Callahan et al., 2016), and show higher mortality (Veach et al., 2020). These historical contingencies constrain microbial responses to changes in the environment, which could shape the trait distribution of the microbial community as a whole.

While the adaptive loss of function, gene transfer, and genome streamlining have diluted trait-linkage to phylogeny in many cases, several functional traits still exhibit taxonomic conservatism (Martiny et al., 2015). Such conservation might further explain why bacteria show phylogenetically conserved responses to different disturbances (Amend et al., 2016; Isobe et al., 2019, 2020) and highlights the importance of characterizing microbial community response to a disturbance at a taxonomic level. However, the taxonomic responses of microorganisms to soil drying can be pretty variable. Gram-positive bacteria are generally more drought-tolerant than Gram-negative bacteria (Manzoni et al., 2012; Uhlírová et al., 2005). However, several Gram-negative bacteria, including Acidobacteria, Verrucomicrobia, and Alphaproteobacteria, have been observed to tolerate periods of droughts, while Actinobacteria, which are Gram-positive, can be responsive to soil drying (de Vries et al., 2018; Isobe et al., 2020). Gram-positive bacteria possess thick peptidoglycan cell walls, which are the initial barrier to drying and osmotic stress, allowing Gram-positive organisms to maintain activity as water potential declines (Manzoni et al., 2012). Similarly, Ascomycota and Glomeromycota have been observed to be more drought tolerant fungal phyla, whereas fungi in the Mortierellaceae family within the Mucoromycota phylum are drought-sensitive (de Vries et al., 2018). Sordariomycetes and Agaricomycetes in tropical forest soils have increased during decreases in precipitation imparted by throughfall exclusion (Buscardo et al., 2021). However, sufficient distinction remains in phylogenetic data-sets at high taxonomic levels to predict the responses of members of a community based on their life-history traits (Evans and Wallenstein, 2014).

A precipitation throughfall exclusion experiment was constructed to improve understanding of how exacerbated natural variability of rain events in tropical forests will impact soil microbial communities. The throughfall exclusion shelters redirect precipitation away from plots that would have otherwise infiltrated the forest floor and soil. The shelters were placed on four lowland tropical forests in Panama that span a 1 m gradient in mean annual precipitation (from 2335 mm to 3421 mm) and shift the background rainfall and dry-season length at each site. Soils were collected following short- and prolonged throughfall exclusion to measure the microbial community's alpha and beta diversity metrics in control and treatment soils. We use this experiment to test three different hypotheses related to the resistance and resilience of tropical forest communities to hydrological disturbance:

1. Historical contingencies render tropical forest soils sites with lower MAP and longer dry seasons more resistant to throughfall exclusion.
2. A generalizable demographic shift occurs across all sites selecting for Gram-positive over Gram-negative bacteria in response to throughfall exclusion.
3. Fungal communities will be more resistant to disturbance than bacterial communities.

2. Materials and methods

2.1. Site information

This study was conducted in four distinct lowland seasonal forests on the Isthmus of Panama (Fig. 1) that range in rainfall from 2335 to 3421 mm mean annual precipitation (MAP). A detailed description and soil USDA taxonomy classification of these sites have been published recently (Cusack et al., 2018, 2019), and further information is provided in Table 1. This region experiences a monsoonal climate with a short dry season, from December to April. The dry season is longer and stronger at the drier sites toward the Pacific Coast (~150 days, Fig. 1), while the Caribbean Coast experiences greater rainfall and shorter dry seasons (~115 days). During these dry seasons, monthly annual precipitation can fall below 60 mm (Leigh 1999; Leigh et al. 1996). The Isthmus includes great variation in the geological substrate (Stewart et al., 1980), which gives rise to contrasting soil fertility that is uncorrelated with changes in rainfall (Pyke et al., 2001; Turner and Engelbrecht, 2011). We selected four sites across the Isthmus of Panama. The Sherman Crane (SC) site is located in the North of Panama (also known as San Lorenzo), close to the Caribbean coast, with MAP ~ 3421 mm of yearly rainfall in 2020. Two sites (P12 and P13) are located on Buena Vista Peninsula and receive the same MAP of ~2590 mm. The final site, Gigante, receives ~2335 mm per year. Three of the forests are on infertile, strongly weathered soils (SC, P12, and GIG), while the P13 site is located on fertile soils with higher base cations, phosphate, and ammonium concentrations than the other three sites (Table 1). This site is situated within close proximity to P12 and thus serves to clarify the role nutrient availability plays in the microbial response to hydrological perturbation.

2.2. Field throughfall exclusion experiment

Throughfall exclusion structures were erected in each of the four Panamanian forests described above. Briefly, 10m × 10m throughfall exclusion plots were paired with similar 10m × 10m control plots, forming one block. Four blocks per site were assigned according to local topography, spatial proximity, and tree cover. Throughfall exclusion structures were designed to cover the whole plot but uses a

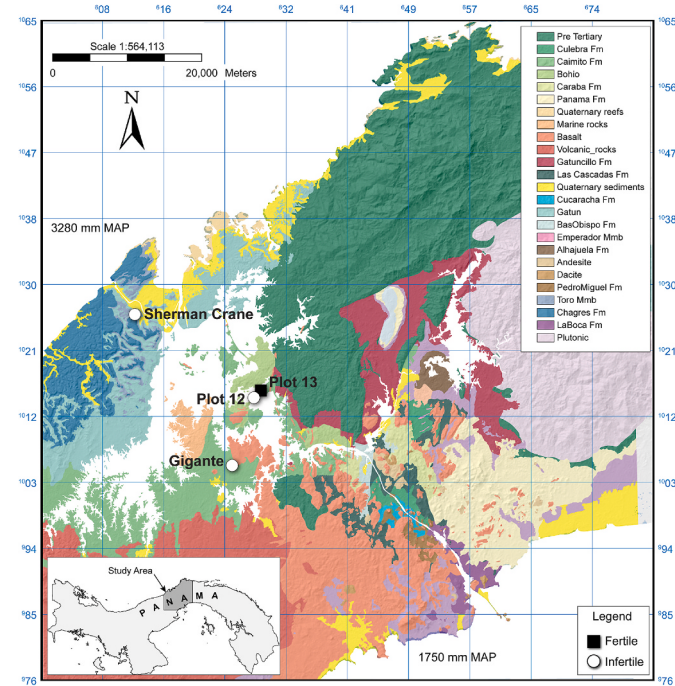


Fig. 1. Location of field sites with varying MAP and fertility in Panama.

Table 1

Characteristics of sites sampled. The mean annual temperature across sites is 26 °C. Mean values and standard deviation provided are from the 0–10 cm depth with n = 4. Total nitrogen, total organic carbon, biomass, ammonium (NH_4^+), inorganic phosphate (PO_4^{3-}), and soil pH were measured from samples collected in January 2020 after long-term throughfall exclusion. For ammonium (NH_4^+) and inorganic phosphate (PO_4^{3-}), entries that are not significantly different share a letter.

Site	Soil Taxonomy	Lat	Long	MAP mm	Dry Season days	Treatment	Total Nitrogen %	Total Organic Carbon %	Total Microbial Biomass nmol per g of SOC	NH_4^+ mg per kg soil	PO_4^{3-} ng per kg soil	pH
Sherman Crane (SC)	Typic Kandidox (Oxisol)	9° 16' 51.132"	-79° 58' 28.9194"	3421	120	Control	0.40(±0.08)	5.82(±1.49)	4516(±810)	1.06 ^a (±0.99)	98 ^a (±30)	4.82(±0.25)
						Exclusion	0.32(±0.16)	4.55(±2.69)	4987(±1934)	0.458 ^a (±0.24)	77 ^a (±27)	5.02(±0.53)
Buena Vista Península P12	Typic Haplolumult (Ultisol)	9° 10' 45.696"	-79° 49' 46.5594"	2595	133	Control	0.36(±0.01)	4.46(±0.19)	4770(±1807)	2.23 ^b (±0.85)	97 ^a (±18)	5.63(±0.31)
						Exclusion	0.40(±0.05)	5.05(±0.70)	5171(±780)	2.43 ^a (±1.42)	153 ^a (±137)	5.85(±0.43)
Buena Vista Península P13	Mollie Oxyequic Hapludalf (Alfisol)	9° 11' 16.3674"	-79° 49' 15.59394"	2590	130	Control	0.48(±0.04)	5.36(±0.44)	4860(±1218)	11.99 ^a (±4.03)	942 ^a (±458)	6.19(±0.27)
						Exclusion	0.40(±0.07)	4.34(±0.88)	4687(±1438)	15.36 ^b (±3.71)	761 ^a (±760)	6.25(±0.34)
Gigante (GIG)	Typic Hapludox (Oxisol)	9° 5' 57.084"	-79° 51' 14.39394"	2335	137	Control	0.40(±0.07)	4.36(±0.85)	4236(±864)	1.30 ^a (±0.30)	937 ^a (±918)	5.65(±0.24)
						Exclusion	0.39(±0.11)	4.06(±1.14)	5162(±683)	2.17 ^a (±0.40)	41 ^a (±49)	5.59(±0.30)

discontinuous design with plastic slats. The slats are equally distributed across the plot with a gap in between to divert ~50% of natural rainfall throughfall away from the plots, reducing the precipitation that reaches the soil. Each plot was trenched to 50 cm, and the trenches were lined with heavy plastic and backfilled with soil (Dietterich et al., 2022). This was done to prevent water diffusion and inhibit roots from leaving the throughfall exclusion plots to forage for water. Throughfall exclusion frames were constructed of aluminum support poles and PVC cross-supports, with a peak in the center of the plots. These structures were topped with clear plastic laminates to cover 50% of the plot area. The roof sloped from a height of 2.3 m to about 1.1 m over a horizontal distance of about 6 m, producing a slope of about 11.3°. Due to the difficulty of installing this experiment, the terms short and long differ in their meaning depending on the site. The wet and intermediate sites (Sherman Crane: 3421 mm, P12: 2595 mm, and P13: 2590 mm) underwent treatment for nine months (short-term) and 18 months (prolonged). However, throughfall exclusion was started six months later at the drier Gigante (2335 mm) site, meaning the short and long-term periods are 3 and 12 months, respectively.

For this study, we sampled soils in May 2019 (short-term throughfall exclusion) and again in January 2020 (prolonged throughfall exclusion). The May time point corresponds to the early wet season, while the January time point corresponds to the beginning of the dry season in Panama. For each sampling effort, we collected soil samples from control and throughfall exclusion plots at two depths (0–10 cm and 10–20 cm) using a 2.54 cm diameter soil corer that was cleaned after each collection. Six sample cores were collected at each depth within each plot and stored in sterile Whirl-Pak bags resulting in 384 cores. The six replicate soil cores for each plot were split and pooled into two composite bags in the field to integrate across spatial heterogeneity per plot at each depth. This resulted in two composite samples per plot at each depth. Soil samples were shipped overnight to Lawrence Berkeley National Laboratory at ambient temperature. The soil composites were separated for biological and chemical analyses and stored at -80 °C.

2.3. Physical and chemical determination of soil properties

Soils for available nutrient analyses were slowly thawed for two days in an -20 °C freezer and then at 4 °C to minimize cell lysis. Thawed soils were shaken in a 1M KCl solution at ratios of 1.0 g of soil per 5 mL of solution for an hour. The extract was filtered through no.45 Whatman filters. Available extractable nutrient concentrations within the filtrate were measured in microplates using sodium salicylate assay for ammonium and malachite green assay for inorganic phosphorus (Lajtha and Jarrell, 1999; Weatherburn, 1967). Base cations and metals were analyzed by Inductively Coupled Plasma Mass spectrometry (Dionex ICS-2100, Thermo Scientific, USA). Gravimetric soil moisture was calculated by collecting field moist soil samples and weighing them before and after drying in a 105 °C oven until weight stabilized. Bulk density measurements used a 1.5" diameter constant volume corer (AMS Inc, American Falls, ID, USA, part 404.39). Bulk density measurements were used to convert soil moisture to volumetric water content (VWC). For pH, 8.0 ± 1.0 g of soil was weighed, mixed with 40 ml of DI water, allowed to settle for approximately 30 min, and the pH of the resulting slurry was measured with a pH meter (SevenCompact pH/Ion meter S220, Mettler Toledo, Columbus, OH, USA). Total organic carbon (TOC) and total nitrogen (TN) were measured using a Costech ECS 4010 elemental analyzer. All soils had a pH below 7.0, and we did not detect any inorganic carbon; thus, TC concentrations are assumed to represent the TOC concentrations. Soil samples for soil moisture were taken at the time of collection for microbial analysis.

2.4. Biological analyses

In order to ascertain the impact of throughfall exclusion on the microbial community (i.e., bacteria, archaea, and fungi), we used a

combination of phospholipid fatty acid biomarker quantification and amplicon sequencing to determine alpha and beta diversity metrics.

2.4.1. Microbial PLFA-derived biomass

Phospholipid fatty acid analyses (PLFA) were measured from lyophilized soil samples to determine the relative total microbial biomass and the biomass of specific microbial groups according to a previously published approach using fatty acid biomarkers (Bouskill et al., 2013; Buyer et al., 2012; Frostegård et al., 2011). Both the prokaryotic and fungal communities sampled in the present study were from the bulk soil and not directly from the rhizosphere or litter layer. PLFAs were measured using gas chromatography-mass spectrometry (Microbial ID, Newark DE). Fatty acid biomarkers used for high-throughput analysis were the same as Buyer et al. (2012). Gram-positive bacteria markers included iso and anteiso-saturated branched fatty acids, while the Gram-negative markers included monounsaturated fatty acids and cyclopropyl 17:0 and 19:0. The 10-methyl fatty acids were markers for Actinobacteria. Fungal biomarkers included the sum 18:2 ω 6 cis and 18:1 ω 9c and removed Arbuscular Mycorrhizae fungal 16:1 ω 5c marker. Fatty acid 18:2 ω 6 cis biomarker was also included since it may be a good indicator of fungi in forest soils (Frostegård et al., 2011). The total PLFA-derived biomass, in nmol per gram soil, was further normalized by the concentration of total organic carbon (TOC) in each sample.

2.4.2. DNA extraction and amplicon sequencing

Total genomic DNA was extracted from 0.25g of each soil sample in duplicate using the DNeasy PowerSoil kit (QIAGEN) following the manufacturer's instructions. The duplicate DNA extractions were combined before PCR amplification and normalized to 10 ng/ μ L. The 16S rRNA gene and ITS region were amplified for the identification of bacteria and archaea, and fungi, respectively. The forward and reverse PCR primers (515F-806R for 16S and ITS1F-ITS2R for ITS) were modified to include Illumina Nextera adapters and 12-bp Golay barcodes were added to the reverse primers as well (Quince et al., 2011; Parada et al., 2016). The PCR reactions were performed in triplicates in 25 μ L reactions with the following reagents: Takara Ex Taq (0.025 units μ L $^{-1}$), 1X Takara Ex Taq PCR buffer, Takara dNTPs mix (200 μ M), Roche bovine serum albumin (0.56 mg mL $^{-1}$), PCR primer (200 nM) and approximately ten ng μ L $^{-1}$ DNA template. 16S gene amplification was performed with the following thermocycler settings, 95 °C for 3 min, 25 cycles of 95 °C for 45 s, 50 °C for 60 s, and 72 °C for 90 s with a final extension of 10 min at 72 °C, whereas the ITS region amplification was done at 95 °C for 3 min, 30 cycles of 95 °C for 30 s, 51 °C for 30 s, and 72 °C for 30 s with a final extension of 5 min at 72 °C. The PCR product triplicates were composited and purified using Sera-Mag (Thermo Scientific) Solid-Phase Reversible Immobilization (SPRI) paramagnetic beads. Quantification of the purified PCR products was done using the Qubit hs-DS-DNA kit (Invitrogen) and pooled in equimolar concentrations (10 ng/ μ L for 16S and 20 ng/ μ L for ITS) and sequenced on a single lane for 300 bp paired-end Illumina v3 MiSeq sequencing completed at the Vincent J. Coates Genomics Sequencing Laboratory at the University of California, Berkeley.

2.4.3. Microbial community composition analysis

Raw amplicon sequences were demultiplexed, trimmed, filtered by quality, and resolved into amplicon sequence variants (ASV) using the DADA2 package v.1.9.1 (Callahan et al., 2016) package in R studio software v.1.1.463 (Team, 2016). Taxonomy was assigned using the Silva reference database (v.132) for 16S and the UNITE database for ITS sequences (Nilsson et al., 2019; Quast et al., 2013). A phylogenetic tree was constructed using the inferred ASVs *de novo* by performing multiple alignments using the DECIPHER R package (v. 2.14.0) and constructed with phangorn package v. 2.5.5 (Schliep, 2011; Wright, 2015). The phylogenetic data was imported into the phyloseq (1.30.0) package to store and analyze the ASV table and the phylogenetic tree (McMurdie

and Holmes, 2013). The workflow resulted in 83 archaeal, 10,133 bacterial, and 8525 fungal ASVs. The total number of reads was converted to relative abundance by dividing the counts of a taxon by the sum of taxon counts across the samples to calculate beta-diversity.

2.5. Statistical analysis

Differences in PLFA-derived biomass and chemistry between sites and treatment were tested using a linear mixed effects model using the R-packages lme4 (Bates et al., 2015), lmerTest (Kuznetsova A. et al., 2017), and MuMIn (Barton, 2022). The fixed effect variables were Site and Treatment, and Block was the random effect in the model. Significant differences across sites and between treatments were tested by calculating the estimated marginal means from the best model (Lenth 2022). Community richness and evenness (Shannon and Inverse Simpson) were calculated across the four forests and between the control and treatment plots. The beta diversity was visualized through a Double Principal Coordinate Analysis (DPCoA (Fukuyama et al., 2012; Pavone et al., 2004; Purdom, 2011), that uses the square root of the cophenetic/patristic distance between ASVs to generate the Euclidean dissimilarity matrix. Euclidean distance measurement considers phylogenetic distances and abundance in our analysis that is robust to noise (Fukuyama et al., 2012). We decided not to use Bray-Curtis which only considers relative abundance without including the phylogenetic distances. Subsequently, differential abundance testing was used to identify and quantify the ASV phylotypes that drive (a) site-to-site variance and (b) the control-to-treatment differences. We used the DESeq2 program (v.1.26.0) for differential analysis of count data to model the dispersion abundances using geometric means for each ASV (Love et al., 2014). ASVs that showed statistically significant positive or negative shifts in abundance between treatments were identified by calculating the binary logarithm fold change ($\log_2\text{foldchange}$) of median counts of the control versus the treatment variable. For significance testing, we used the Wald test with Benjamini and Hochberg adjusted P-values. Variance partitioning approaches, including permutational multivariate analysis (PERMANOVA) and canonical component analysis (CCA), were applied to relate phylogenetic shifts to changes in soil moisture or chemistry through DPCoA distance measurements. PERMANOVAs were run on the DPCoA distance matrices using the adonis function in the vegan package v.2.5-7 (Oksanen and Others, 2011). PERMDISP was employed to determine if the significant differences were driven by dispersion or centroid in beta diversity PERMANOVA. Tree-based visualizations of relative abundances for taxa identified in the samples were done using Metacoder v.0.3.4 ((Foster et al., 2017)). Heat trees were generated and used binary log ($\log_2\text{foldchange}$) ratios of the median counts for each taxon and used the Wald test within the Metacoder program with Benjamini and Hochberg adjusted P-values. P12, P13, and GIG control plots were compared to SC control plots for tree comparisons across sites. Metacoder Trees showing comparisons between treatments within the site were also generated.

3. Results

3.1. Physicochemical factors

Within control plots across the four sites on January 2020, we observed soil moisture content (measured as VWC) to decrease from the wettest site, SC (3421 mm), to the driest, GIG (2335 mm) (Fig. S1). TOC and TN in the topsoil did not vary significantly across the four forest soils. TOC was between 4.0 and 5.8% by weight and 0.32–0.47% for TN (Table 1). Ammonium concentrations were low in the infertile sites (0.46–2.43 mg NH $^+$ kg soil) and significantly higher in the fertile, mid-rainfall site, P13 (2590 mm) (~12.0–15.4 mg NH $^+$ kg soil). Similarly, phosphate was also higher in P13 sites and low at the three other sites except for control plots in GIG (Table 1). Yet phosphate concentrations were highly variable in P13 plots, ranging from undetectable amounts to

500 ng PO₄³⁻ per kg of soil (Fig. S2). SC sites had the lowest average pH below 5.0 while P13 plots had an average pH above 6.0 (Fig. S3).

When comparing control soils with throughfall excluded soils, we observed a general increase in TOC and TN at the mid-MAP sites, P13 and P12, following prolonged throughfall exclusion, but a decline in exclusion plots at SC and GIG. Average ammonium concentration at the P13 (2590 mm) exclusion plots did slightly increase compared to average concentrations in the P13 control plots. Bulk measurements of soil moisture (i.e., VWC) showed no significant differences between the control and throughfall exclusion plots after prolonged exclusion (Table S1).

3.2. Microbial community structure across sites

Below, we describe the PLFA data and the alpha and beta diversity metrics emerging from the microbial analyses. We initially contrast the control sites across the MAP gradient to ascertain how these communities are structured before subsequently moving on to describe a cross-gradient response to throughfall exclusion.

The PLFA-derived biomass of the microbiota across these soil plots are largely dominated by bacteria, which compose between 34 and 47% of the total PLFA-derived biomass within the control plots. Across the four sites, there were no significant differences in total and fungal biomass (Fig. 2a and b). By contrast, the biomass of different bacterial groups increased significantly with decreasing MAP. The biomass of the Actinomycetes, the Gram-negative and Gram-positive bacteria were ~53%, ~131%, and ~127% higher at the drier GIG (2335 mm) site relative to the SC (3421 mm) soils with the highest MAP (Fig. 2c, d, e). We also observed site explained variance in the biomass of Gram-negative and Gram-positive bacteria at the mid-rainfall site P12 when compared to SC.

'Site' was a significant predictor of community structure (PERMANOVA p = 0.001). Average taxonomic richness and evenness generally increased for prokaryotes with decreasing MAP (Fig. S4). Overall, the major prokaryotic taxa dominating these soils were the Proteobacteria, Acidobacteria, Actinobacteria, and Verrucomicrobia. Phyla present but

at smaller relative abundances included the Bacteroidetes, Rokubacteria, Chloroflexi, Nitrospirae, and Entotheonellaeota (Fig. S5). The relative abundance of the Acidobacteria decreased with decreasing MAP, while the Actinobacteria increased with decreasing MAP. Relative abundance of Verrucomicrobia was lowest at GIG (2335 mm), intermediate at SC (3421 mm), and greatest at the mid-range P12 and P13. The relative abundance of Proteobacteria was greater in P13 than in the other sites. Nanoarchaeaeota generally increased in relative abundance with decreasing MAP. Fig. 3a shows a DPCoA, a phylogenetic distance-based ordination, depicting the relative dissimilarity between the different sites under short and prolonged throughfall exclusion. The sites with the most dissimilar microbial communities were SC and P13 (2590 mm) at both time points. The dissimilarity between sites across the primary axis accounts for 49.9% of the variance after short-term exclusion and 52.4% after prolonged exclusion (Fig. 3).

The differential abundance analysis highlights which phyla are significantly enriched in the SC control relative to the other control plots across the rainfall gradient. Compared to the other sites, there was a significant decrease in Acidobacteria at the wettest site SC (Fig. S6). But control plots in P12 (2590 mm), P13, and GIG were significantly enriched in Actinobacteria, including members of the Frankiales, Coryn bacteriales, and Gaiellales order (Fig. S8). Significant enrichment of ASV from Lactescibacteria, Rokubacteria, and Gemmatimonadetes was also observed in control plots from P12, P13, and GIG when compared to counts from SC (Fig. S8).

Fungal communities were dominated by Ascomycota, Basidiomycota, and Mortierellomycota and showed little site-to-site variability (Fig. S6). Fungal richness and evenness were highest in P13 and lowest in GIG (Fig. S5). The relative abundance of Ascomycota increased from SC to P13 (Fig. S7) but declined at GIG. The relative abundance of Basidiomycota was lowest at P12 and highest at P13, whereas the Mortierellomycota decreased in relative abundance along with decreasing MAP. We note that beta diversity measurements in fungal communities did not clearly differentiate the sites (p = 0.114; Fig. S7; Table S3).

A canonical correspondence analysis (CCA) was used to determine

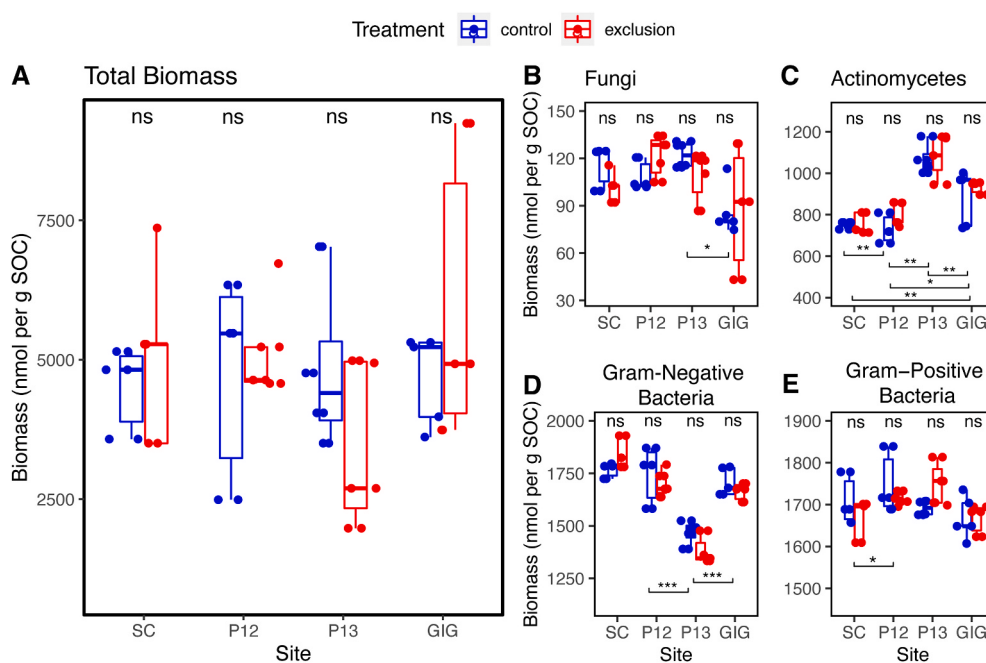


Fig. 2. Microbial biomass determined from phospholipid fatty acid analysis from the top horizon (0–10 cm) from samples taken after prolonged treatment. Whiskers indicate the minimum and maximum biomass values. Sites are Sherman Crane (SC - 3421 mm), Buena Vista Peninsula Site 12 (P12 - 2590 mm) and 13 (P13 - 2590 mm), and Gigante (GIG - 2335 mm) site. Total biomass was normalized by total organic carbon (TOC) content. Control plots are indicated in blue, while biomass from exclusion plots is indicated in red. Biomass is separated by microbial type: (b) Fungi, (c) Actinomycetes, (d) Gram-negative and (e) Gram-positive bacteria. The biomass reported is from the topsoil (0–10 cm) since throughfall exclusion had more discernible impacts on this depth range relative to the subsoil (10–20 cm). The statistics used were linear mixed effect models and comparing marginal means. Significance of site and treatment variables explaining biomass with block as a random effect are indicated by asterisks under boxplots. Treatment significantly explaining biomass is indicated above boxplots. Asterisks indicate the magnitude of p-values of <0.05(*), <0.001 (**), and <0.0001 (***) (For interpretation of the references to color in this figure legend, the reader is referred to the Web version of this article.)

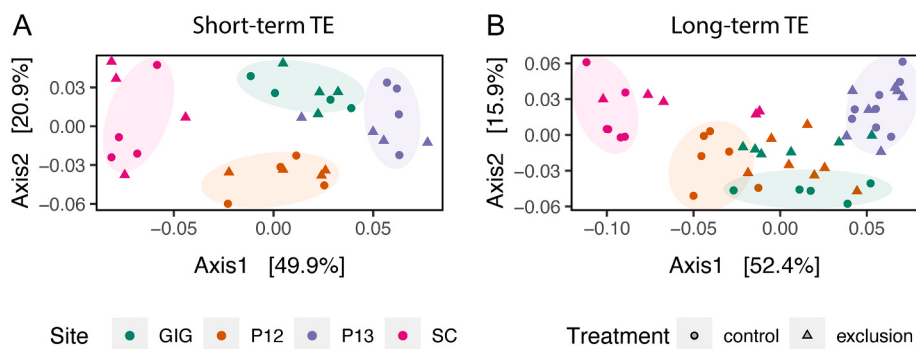


Fig. 3. Double Principal Coordinate Analysis (DPCoA) of Bacteria and Archaea after A) short-term and B) long-term partial throughfall exclusion. Control plots are in circles, and exclusion plots are in triangles. Green symbols indicate Gigante (GIG-2335 mm) points. P12 (2595 mm) points are indicated in brown, and P13 (2590 mm) are purple symbols. The Sherman Crane (3421 mm) samples are indicated in pink. Ellipses highlight the clustering of samples within control plots at a specific site. (For interpretation of the references to color in this figure legend, the reader is referred to the Web version of this article.)

which environmental variables best explained the changes in microbial community composition across sites. CCA analysis using the DPCoA distances clustered prokaryotic communities primarily by site (Fig. 4a). For bacteria and archaea, the primary axis explained 46.2% of the variance across the data. A number of environmental variables were significant factors in the emergent community structure (PERMANOVA $p = 0.001$; Table S4), including soil moisture and Fe, which were the main factors discriminating between communities at the wettest site SC from the other sites. The dissimilarity of P13 (2590 mm) from the other sites was predominantly explained by soil fertility (TN, ammonium, base cations) and pH. Finally, total microbial PLFA-derived biomass, inorganic phosphate, and sodium concentrations distinguish prokaryotic communities at the drier site, GIG, and the mid-rainfall infertile site, P12. However, the collected environmental variables were unable to explain the emergent fungal community structure as measured by DPCoA distances across sites (Fig. 4b; Table S4).

3.3. Impacts of throughfall exclusion on microbial biomass and community composition

Throughfall exclusion imparted no significant effect on PLFA-derived total biomass (Fig. 2a), but clear trends emerged (Table S2) when separated by the domain (i.e., fungi and bacteria) or cell-wall morphology (i.e., Gram-negative and positive). However, PLFA-derived fungal biomass showed a clear decline under throughfall exclusion at the wettest site SC and the P13 and a general drop at the driest site GIG. PLFA-derived biomass at P12 increased (Fig. 2b). Gram-negative and Gram-positive bacterial biomass both increased during

throughfall exclusion at the wettest sites (SC) and driest sites (GIG) but decreased at the mid-rainfall sites (P12 and P13, Fig. 2d and e). Actinomycetes also showed qualitatively similar trends, with throughfall exclusion promoting higher average PLFA-derived biomass at the SC and GIG sites but a negligible impact at the P12 and P13 sites. Taken together, these data suggest that, despite not impacting total biomass, throughfall exclusion reshaped community abundance and composition.

Following short-term treatment, no significant differences were observed between microbial communities' richness, evenness, or composition when comparing control and throughfall exclusion plots at each site (Fig. S4; Fig. 3a). However, after prolonged throughfall exclusion, the beta diversity metrics demonstrated an increasing dissimilarity in community composition in treatment relative to controls plots. This effect was confined to the infertile sites (i.e., SC, P12, and GIG) and, when considered with the aforementioned alpha diversity metrics, is indicative of shifts in the relative abundance of different taxa (Figs. 3b and 4). The dissimilarity between the community composition of control and throughfall excluded plots was strongest at the P12 site, which diverged across the primary ordination axis. However, we also noted similar dissimilarity between control and treatment plots at the GIG site, which separated across the secondary axis, and converged towards a very similar community composition as that emerging under treatment at the P12 plots. The SC prokaryote community in the exclusion plots began to show greater similarity to the community composition at P12 and GIG exclusion plots (Fig. 3b). By contrast, the community composition of bacteria and archaea at the nutrient-rich site (P13) showed no divergence from the control site following prolonged treatment (Fig. 3b).

The observed shifts in community composition under throughfall exclusion were attributable to the significant enrichment of multiple taxa across the different sites ($p < 0.05$, Fig. 5). Within some sites, a phylogenetic signal was discernible amongst the enriched phyla. For example, the Nitrospirae (*Nitospira*), Chloroflexi (*Anaerolineae*), several orders of Proteobacteria, and Entotheonella (*Entotheonellaeota*) were enriched following throughfall exclusion within both the SC (3421 mm), P12 (2595 mm), and GIG (2335 mm) plots (Fig. 5; Fig. S8). Similarly, members of the Bacteroidetes (e.g., *Chitinophagales*) and Proteobacteria were significantly enriched under throughfall exclusion at both the P12 and SC sites (Fig. 5). Actinobacteria, Planctomycetes, and Verrucomicrobia were only significantly enriched following throughfall exclusion in P12 (Fig. 5). Interestingly, members of the Bacteroidetes and Proteobacteria (*Xanthomonas* and *Myxococcales*) were enriched both in exclusion plots in SC and control plots in GIG. Distinct archaeal taxa were enriched in exclusion plots at different sites. At the mid-rainfall site P13, the relative abundance of the Thaumarchaeota was much higher in exclusion plots than in control plots, while Nanoarchaeaeota were enriched in the SC exclusion plots relative to the corresponding control plots. By contrast, we observed no discernible impact on fungal community structure relative to the control plots (Fig. S7) and little discrimination of sites when the measured edaphic drivers were accounted for (Fig. 4b).

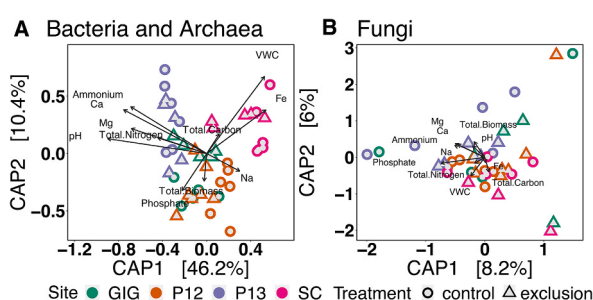


Fig. 4. Canonical correspondence analysis (CCA) plots of samples taken in January 2020 after long-term partial throughfall exclusion was applied to relate phylogenetic responses to changes in soil moisture or chemistry. Dissimilarity matrices were distances calculated by Double Principal Component analysis (DPCoA). Variables used for the model are total organic carbon (TOC), total nitrogen (TN), Ammonium concentration, inorganic phosphate (phosphate), total microbial biomass (total biomass), Volumetric water content (VWC), iron (Fe), magnesium (Mg), calcium (Ca), and soil pH. Circle symbols indicated samples from control plots and triangle symbols for exclusion plots. Arrows in CCA are significant factors for bacteria and archaea (PERMANOVA $p = 0.001$) but not fungi.

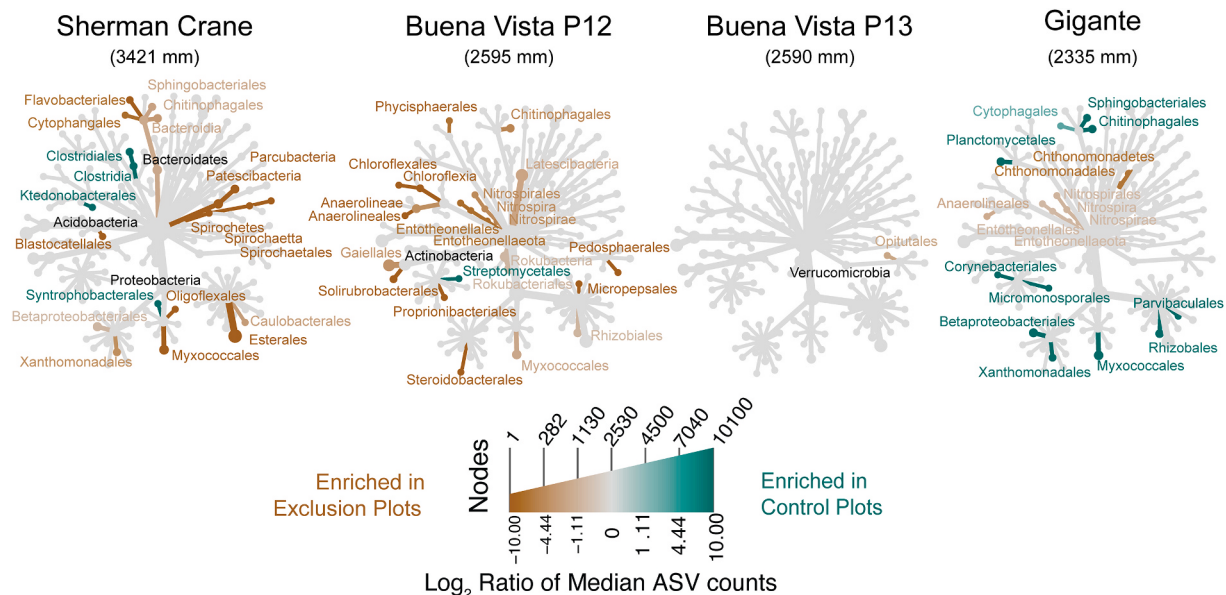


Fig. 5. Tree-based visualizations for taxa identified in samples. Colors indicate the \log_2 ratios of median counts between control and exclusion plots. Brown colors indicate taxa enriched in control plots, while green colors indicate taxa enriched in exclusion plots. Trees are separated by the site. Colored branches indicate taxa significantly enriched in plots ($p < 0.05$ Wald test). (For interpretation of the references to color in this figure legend, the reader is referred to the Web version of this article.)

Finally, we used CCA to identify the environmental factors underpinning shifts in community composition within the site as a result of throughfall exclusion in infertile soils (Fig. S9). This analysis revealed a strong relationship between soil moisture (volumetric water content VWC) and ammonium concentrations at the drier GIG exclusion plots ($p = 0.007$; Table S5). For communities within the mid-rainfall P12 throughfall exclusion plots, separation from the control plots was associated with increasing TC, TN, Mg, Ca, and soil pH. In comparison, communities in exclusion plots at the wettest site SC were associated with changing pH and Ca. Despite the site-to-site divergence in factors influencing the composition of throughfall exclusion plots, it was clear that total carbon and nutrients, including total nitrogen and phosphate, were essential factors structuring microbial community composition in the control plots at SC and GIG, whereas soil moisture was the most important factor associated with community composition within the P12 control plots.

4. Discussion

4.1. Bacterial and archaeal responses to throughfall exclusion

The taxonomic composition of microbial communities shows a profound sensitivity to disturbance (Shade et al., 2012) that may (Louca et al., 2018) or may not (Rocca et al., 2018) reshape the functional diversity of a community, and feedback on soil biogeochemistry. As climate changes, the frequency of pulse (e.g., drought) and press (e.g., warming or elevated atmospheric CO₂) disturbances in the tropics will play an increasingly important role in shaping community composition. The sensitivity of tropical soil communities to the impact of multi-faceted climate change is generally understudied. Tropical microbial communities have previously been shown to be sensitive to warming (Nottingham et al., 2020) and soil drying (Bouskill et al., 2013). However, the factors that regulate a community's sensitivity relative to its resistance remain poorly understood. Here we show that prolonged throughfall exclusion imparted remarkably divergent responses across the study sites. The extent to which bacterial and archaeal communities shifted under treatment was broadly dependent on (a) soil fertility and (b) the length of the dry season and MAP.

4.1.1. High nutrient availability buffers the impact of throughfall exclusion

Shifts in bacterial and archaeal community diversity under throughfall exclusion occurred solely within soils that were relatively low in bedrock-derived and atmospherically-deposited nutrients. Throughfall exclusion was associated with strong shifts in community structure in all three infertile sites studied but no discernible shift in the fertile site. In this case, the availability of soil nutrients could either sustain a metabolic response within the community to resist the ongoing perturbation or facilitate the rapid recovery of the initial community following the onset of perturbation (Bardgett and Caruso, 2020).

As soils dry, shrinking water films can concentrate solutes, which can impart stress on microorganisms (Malik and Bouskill, 2022; Schimel, 2018). In response to matric and osmotic stressors, microorganisms have been shown to increase demand for both nitrogen and phosphorus (Buscardo et al., 2021), alter the composition of phosphorus-rich cell walls (Williams and Rice, 2007) to maintain cellular turgor, and synthesize a range of compatible solutes to maintain macromolecular integrity during this stress (Bremer and Krämer, 2019). These compounds include a range of non-structural carbohydrates and amino acids high in nitrogen and, in some cases, phosphorus. However such a metabolic response to stress is energetically expensive (Oren, 1999) and likely only used when substrate availability is sufficient to cover the energetic and macromolecular cost of synthesizing these compounds (Manzoni et al., 2014). This could certainly be the case at the mid-rainfall, fertile P13 site, which shows higher carbon and nutrient availability relative to the other sites, and provides possible avenues to identify which soil fertility components directly support purported microbial responses to soil drying and shifts in rainfall variability.

Such nutrient-enabled community resistance to soil throughfall exclusion in tropical forest soils may hold if nutrient concentrations do not become severely limited. However, throughfall exclusion and drought in tropical forest soils can bring about a drop in phosphorus availability (Bouskill et al., 2016; O'Connell et al., 2018), as fluctuating soil redox potential under drying increases phosphorus sorption to soil minerals. Therefore, prolonged soil drying under a changing climate may potentially restrict the metabolic response of the microbial community by reducing nutrient availability.

4.1.2. Impacts of historical contingency on community response to throughfall exclusion

In contrast to the resistance observed at the fertile soil site (P13), the comparatively infertile sites across the rainfall gradient (SC, P12, and GIG) showed shifts in microbial community composition following prolonged throughfall exclusion. The GIG and P12 sites exhibited a ‘treatment microbiome,’ whereby an overlapping community composition emerged under throughfall exclusion. This shift at GIG occurred under a much shorter time scale due to the six-month delay in constructing the throughfall shelters at this site, emphasizing that this drier site appeared pre-conditioned to the environmental shifts imposed by the treatment. Such a strong and complementary response to throughfall exclusion at GIG and P12 sites is interesting when contextualized by the lack of measurable differences in soil moisture within control and throughfall exclusion. Microbial community composition has previously been shown to be more sensitive to disturbance impacts than bulk soil properties (Ma et al., 2019), and in this case, community composition appeared more sensitive to perturbation than bulk measurements of water content at the plot scale. One reason that significant changes in VWC were not observed could be the high C and clay texture of these soils. Finer textures enhance the transport of water from deeper in the profile through capillary rise, while high C enhances moisture retention. Thus, bulk measurements may not capture disturbance without quantifying additional factors such as matric potential and soil pore structure. Since microbes are sensitive to matric potentials (Manzoni et al., 2012), microbial community shifts may be a more sensitive indicator of disturbance than VWC. The emergence of this treatment microbiome might reflect the lower MAP and longer dry seasons at GIG and P12, which could condition it to respond quickly, and to a degree, predictably to rainfall perturbations.

Historical contingencies did factor into determining resistance to disturbance but, as discussed above, are outweighed by fertility. Throughfall exclusion at the P12 (2595 mm) and GIG (2335 mm) sites selected for taxa that have been observed to respond positively to soil drying. For example, the observed enrichment in Gram-positive bacteria in throughfall exclusion plots, such as Actinobacteria, might be expected due to the morphological and physiological traits of this group, including the ability to sporulate under adverse environmental conditions (Jordan et al., 2008; Mayfield et al., 1972). Moreover, Gram-positive bacteria within the Actinobacteria also possess a large secondary metabolome that plays a role in conferring resistance to environmental stress (Wolf et al., 2013). In addition to producing compatible solutes, some taxa use filamentous structures to extend their growth during low soil moisture conditions (Wolf et al., 2013). These traits likely explain an overall negative trend with soil moisture of the Actinobacteria (Chanal et al., 2006), and an elevated relative abundance in dry soils (Bachar et al., 2010), and under throughfall manipulation experiments in the tropics and subtropics (Bouskill et al., 2013; Zhou et al., 2019).

While the elevated relative abundance of different Gram-positive organisms might be predicted on the basis of their ecology and physiology, we also note an increase in the relative abundance of a number of Gram-negative taxa at throughfall exclusion plots. For example, we observed the statistically significant enrichment of members of the Acidobacteria phyla under throughfall exclusion across all three infertile sites (GIG, P12, SC). The increased relative abundance of Acidobacteria has been observed in drying manipulations in field and microcosm experiments with tropical and subtropical forest soils (Bu et al., 2018; Supramaniam et al., 2016). A positive response to drying could be facilitated by the metabolic capacity of some Acidobacteria to produce cellulose, and exopolysaccharides and form biofilms under osmotic stress, such as detected in *Komagataeibacter* (Kielak et al., 2017; Ward et al., 2009). Furthermore, members of the large Proteobacteria phylum also increased in relative abundance in the P12 and GIG treatment plots. This is consistent with previous precipitation manipulation experiments in tropical soils, which have observed the enrichment of Alpha- or

Betaproteobacteria (Bouskill et al., 2013; Nemergut et al., 2010). In addition, we also show here an increase in the relative abundance of the Delta- and Gammaproteobacteria in tropical forest soils from throughfall exclusion plots when compared to control plots within a site. However, while not necessarily predicted to increase under soil drying, some taxa within the Proteobacteria phyla show the capacity to avoid osmotic and matric stress associated with drought by increasing biofilm production (Römling and Galperin, 2015). Proteobacteria observed to possess traits for biofilm formation have been found within the Alpha-, Beta-, and Gamma-proteobacteria, and more specifically within the genera *Gluconobacter*, *Burkholderia*, *Pseudomonas*, *Xanthomonas*, and *Dickeya* (Ross et al., 1991; Ude et al., 2006; Freitas et al., 2011; Römling and Galperin, 2015). Biofilm production protects embedded cells from rapid fluctuations in external water potential (Flemming et al., 2016), increasing their relative abundance within the community as mortality reduces the abundance of other non-biofilm forming groups. Yet many of our observed enriched taxa classified to the family and genus level did not fall into the genera mentioned above. However, given that the capacity for producing EPS is distributed widely across different taxa (Flemming et al., 2016), it is possible that this trait is possessed by these uncharacterized taxa.

Finally, the strong response of Gram-negative bacteria might also represent metabolic cross-feeding between tolerant and vulnerable organisms under increased cell-to-cell interactions as soils dry (Tecon et al., 2018). Organisms that do not invest in the production of osmolytes could ‘cheat’ by assimilating osmolytes from lysed cells, successfully competing with organisms that do. Indeed, opportunistic life-history strategies have been observed in soil microbial communities in response to drying-rewetting cycles (Evans and Wallenstein, 2014); however, further research is required to develop and test this hypothesis.

We observed a less pronounced throughfall exclusion-induced shift in the microbial community at the drier site, GIG. This might be indicative of a community adapted to drier conditions relative to the other sites with higher MAP and, therefore, less sensitive to the imposed disturbance. Seasonal shifts in environmental conditions give rise to dynamic bacterial communities, whereby distinct communities are selected for and recur during specific times of the year (Bouskill et al., 2011; Ward et al., 2017). Such dynamics might explain why GIG, with prolonged dry seasons and lower MAP, showed smaller, more discrete shifts in beta diversity under throughfall exclusion relative to P12. The implication here is that tropical sites that have prolonged annual dry seasons could harbor a prokaryotic seed bank (Lennon et al., 2021) adapted to an increasing intensity of drought, reducing the impact of this perturbation on microbial assembly and function.

We also note that the community emerging under throughfall exclusion treatment at the wetter SC site showed taxonomic similarity with the untreated control soil communities at the drier GIG site (Fig. S7). This suggests that, despite having higher precipitation and shorter dry season length, the SC site harbors organisms with similar life-history traits and responses to drier conditions as those endemic to the GIG site. This emphasizes the control soil moisture availability has on community composition and lends a degree of predictability to how tropical microbial communities could change under rainfall perturbations. We initially hypothesized that there would be demographically generalizable shifts across all sites in response to throughfall exclusion. We expected enrichment of Gram-positive bacteria with a concurrent decrease in Gram-negative bacteria. However, we found no clear morphological signal in response to disturbance, such as a clear divergence between Gram-positive or negative bacteria due to throughfall exclusion.

4.2. Fungal response to throughfall exclusion

Fungal biomass, derived from the PLFA markers, showed a divergent response across the different sites. Biomass declined slightly under

throughfall exclusion at SC (3421 mm) and P13 (2590 mm) but increased at GIG (2335 mm) and P12 (2595 mm). As such, we partially reject our final hypothesis inferring that fungi will be resistant to throughfall exclusion. Recent studies in subtropical forest soils have also highlighted sensitivity within fungal communities to throughfall exclusion conditions, including a decline in biomass consistent with our observations at SC and P13 (Zhang et al., 2021; Zhao et al., 2018). This suggests that drought resistance is not a universal trait within the fungal community. Our contrasting observations at GIG and P12 do fall in line with previous studies demonstrating that fungi are broadly resistant to drought (Evans and Wallenstein, 2012; Six, 2012) and to drying and rewetting cycles (Bapiri et al., 2010; Barnard et al., 2015). This resistance has been attributed to key physiological mechanisms including hyphal networks and mutualism. For example, filamentous structures have been shown to aid fungi in enduring water stress (Freckman, 1986) by transporting water and substrates through the hyphal network (Boer et al., 2005). Moreover, fungi possess drought-resistant traits similar to bacteria, including compatible solute synthesis and EPS production (Crowther et al., 2014).

A caveat to our observation of a decline in fungal biomass is the overall resistance in the composition of the fungal community to disturbance as measured by beta diversity. The lack of a beta diversity response in our study might be attributed to the aforementioned drought-resistant traits, regardless of slight changes in biomass. Our canonical analysis of fungal community composition with environmental variables did not show a strong separation by the treatment that could be attributed to a specific edaphic factor. However, it is possible that a strong fungal response was missed by sampling the bulk soil rather than around the rhizosphere or within litter layers.

In contrast to our observations on fungal beta diversity, previous work has also demonstrated shifts in community composition under soil drying and throughfall exclusion within tropical forest soils (Buscardo et al., 2021; de Oliveira et al., 2020; He et al., 2017). In particular, notable increases in the relative abundance of dark septate and phytopathogenic fungi were observed in tropical forest soils (Buscardo et al., 2021; de Oliveira et al., 2020); while the abundance of Sordariomycetes and Agaricomycetes increased in tropical grassland soils under drought (He et al., 2017). Deviations of fungal community responses to rainfall perturbations within tropical soils could be due to differences in physiochemical properties such as texture, pore structure, and aggregation. These factors could influence the degree of soil moisture variation from throughfall exclusion and other hydrological disturbances.

5. Conclusion

The present study demonstrates seemingly disparate responses of tropical forest soils to partial throughfall exclusion, which were dependent on site-specific climate history (e.g., MAP, dry season lengths). In general, the historical contingencies that shape community composition across a 1 m MAP gradient in tropical forest soils partially determine the level of resistance to throughfall exclusion but are overshadowed by soil fertility. As such, historical contingencies and soil properties (e.g., texture and fertility) need to be accounted for when attempting to predict how tropical soil microbial communities may respond to projected disturbances in the hydrological cycle. Further work must connect the observed shifts in community composition to changes in microbial trait distribution and determine whether community responses to the changing climate will alter the carbon cycle within tropical forest soils.

Declaration of competing interest

The authors report no competing interests.

Data availability

Data reported in this manuscript, and codes used to create the figures have been uploaded to a public repository (<https://ess-dive.lbl.gov>) under doi:10.15485/1874586.

Acknowledgments

Funding for this work was provided by the US Department of Energy, Office of Science (BER), Early Career Research Program to N.J. Bouskill (#FP00005182) and Daniela Cusack (#DE-SC0015898). We thank Biancolini Castro, Lily Colburn, Alexandra Hedgpeth, Jason Brawdy, Korina Valencia, and Carley Tsiames for the help in collecting these samples with us. We thank Wenming Dong (LBNL) for assistance with chemical analysis and Patrick Sorenson (LBNL) for assistance with linear mixed model analysis. Special thanks to the Tupper Soil Lab in the Smithsonian Tropical Research Institute for coordination of sample handling and transport.

Appendix A. Supplementary data

Supplementary data to this article can be found online at <https://doi.org/10.1016/j.soilbio.2022.108924>.

References

- Amend, A.S., Martiny, A.C., Allison, S.D., Berlemon, R., Goulden, M.L., Lu, Y., Treseder, K.K., Weihe, C., Martiny, J.B.H., 2016. Microbial response to simulated global change is phylogenetically conserved and linked with functional potential. *The ISME Journal* 10 (1), 109–118.
- Azarbad, H., Tremblay, J., Giard-Laliberté, C., Bainard, L.D., Yergeau, E., 2020. Four decades of soil water stress history together with host genotype constrain the response of the wheat microbiome to soil moisture. *FEMS Microbiology Ecology* 96 (7). <https://doi.org/10.1093/femsec/fiaa098>.
- Bachar, A., Al-Ashhab, A., Soares, M.I.M., Sklarz, M.Y., Angel, R., Ungar, E.D., Gillor, O., 2010. Soil microbial abundance and diversity along a low precipitation gradient. *Microbial Ecology* 60 (2), 453–461.
- Bapiri, A., Báth, E., Rousk, J., 2010. Drying-rewetting cycles affect fungal and bacterial growth differently in an arable soil. *Microbial Ecology* 60 (2), 419–428.
- Bardgett, R.D., Caruso, T., 2020. Soil microbial community responses to climate extremes: resistance, resilience and transitions to alternative states, 1794. *Philosophical Transactions of the Royal Society of London Series B Biological Sciences* 375, 20190112.
- Barnard, R.L., Osborne, C.A., Firestone, M.K., 2015. Changing precipitation pattern alters soil microbial community response to wet-up under a Mediterranean-type climate. *The ISME Journal* 9 (4), 946–957.
- Bartoń, K., 2022. MuMin: multi-model inference. R package version 1.46.0. <https://CRAN.R-project.org/package=MuMin>.
- Bates, D., Mächler, M., Bolker, B., Walker, S., 2015. Fitting linear mixed-effects models using lme4. *Journal of Statistical Software* 67 (1), 1–48. <https://doi.org/10.18637/jss.v067.i01>.
- Boer, W., de Folman, L.B., Summerbell, R.C., Boddy, L., 2005. Living in a fungal world: impact of fungi on soil bacterial niche development. *FEMS Microbiology Reviews* 29 (4), 795–811.
- Bonan, G.B., 2008. Forests and climate change: forcings, feedbacks, and the climate benefits of forests. *Science* 320 (5882), 1444–1449.
- Bouskill, N.J., Eveillard, D., O'Mullan, G., Jackson, G.A., Ward, B.B., 2011. Seasonal and annual reoccurrence in betaproteobacterial ammonia-oxidizing bacterial population structure. *Environmental Microbiology* 13 (4), 872–886.
- Bouskill, N.J., Lim, H.C., Borglin, S., Salve, R., Wood, T.E., Silver, W.L., Brodie, E.L., 2013. Pre-exposure to drought increases the resistance of tropical forest soil bacterial communities to extended drought. *The ISME Journal* 7 (2), 384–394.
- Bouskill, N.J., Wood, T.E., Baran, R., Hao, Z., Ye, Z., Bowen, B.P., Lim, H.C., Nico, P.S., Holman, H.-Y., Gilbert, B., Silver, W.L., Northen, T.R., Brodie, E.L., 2016a. Belowground response to drought in a tropical forest soil. II. Change in microbial function impacts carbon composition. *Frontiers in Microbiology* 7, 323.
- Bouskill, N.J., Wood, T.E., Baran, R., Ye, Z., Bowen, B.P., Lim, H., Zhou, J., Van Nostrand, J.D., Nico, P., Northen, T.R., Silver, W.L., Brodie, E.L., 2016b. Belowground response to drought in a tropical forest soil. I. Changes in microbial functional potential and metabolism. In: *Frontiers in Microbiology*, vol. 7. <https://doi.org/10.3389/fmicb.2016.00525>.
- Bremer, E., Krämer, R., 2019. Responses of microorganisms to osmotic stress. *Annual Review of Microbiology* 73, 313–334.
- Buscardo, E., Souza, R.C., Meir, P., Geml, J., Schmidt, S.K., da Costa, A.C.L., Nagy, L., 2021. Effects of natural and experimental drought on soil fungi and biogeochemistry in an Amazon rain forest. *Communications Earth & Environment* 2 (1), 1–12.
- Bu, X., Gu, X., Zhou, X., Zhang, M., Guo, Z., Zhang, J., Zhou, X., Chen, X., Wang, X., 2018. Extreme drought slightly decreased soil labile organic C and N contents and

- altered microbial community structure in a subtropical evergreen forest. *Forest Ecology and Management* 429, 18–27.
- Buver, J.S., S, M., Sasser, M., 2012. High throughput phospholipid fatty acid analysis of soils. *Applied Soil Ecology* 61, 127–130. <https://doi.org/10.1016/j.apsoil.2012.06.000>.
- Callahan, B.J., McMurdie, P.J., Rosen, M.J., Han, A.W., Johnson, A.J.A., Holmes, S.P., 2016. DADA2: high-resolution sample inference from Illumina amplicon data. *Nature Methods* 13 (7), 581–583.
- Chadwick, R., Good, P., Martin, G., Rowell, D.P., 2016. Large rainfall changes consistently projected over substantial areas of tropical land. *Nature Climate Change* 6 (Issue 2), 177–181. <https://doi.org/10.1038/nclimate2805>.
- Chanal, A., Chapon, V., Benzerara, K., Barakat, M., Christen, R., Achouak, W., Barras, F., Heulin, T., 2006. The desert of Tataouine: an extreme environment that hosts a wide diversity of microorganisms and radiotolerant bacteria. *Environmental Microbiology* 8 (3), 514–525.
- Crowther, T.W., Maynard, D.S., Crowther, T.R., Peccia, J., Smith, J.R., Bradford, M.A., 2014. Untangling the fungal niche: the trait-based approach. *Frontiers in Microbiology* 5, 579.
- Crowther, T.W., van den Hoogen, J., Wan, J., Mayes, M.A., Keiser, A.D., Mo, L., Averill, C., Maynard, D.S., 2019. The global soil community and its influence on biogeochemistry. *Science* 365 (6455). <https://doi.org/10.1126/science.aav0550>.
- Cusack, D.F., Ashdown, D., Dietterich, L.H., Neupane, A., Ciochina, M., Turner, B.L., 2019. Seasonal changes in soil respiration linked to soil moisture and phosphorus availability along a tropical rainfall gradient. *Biogeochemistry* 145 (3), 235–254. <https://doi.org/10.1007/s10533-019-00602-4>.
- Cusack, D.F., Marksteijn, L., Condit, R., Lewis, O.T., Turner, B.L., 2018. Soil carbon stocks across tropical forests of Panama regulated by base cation effects on fine roots. *Biogeochemistry* 137 (1), 253–266.
- Cusack, D.F., Silver, W.L., Torn, M.S., Burton, S.D., Firestone, M.K., 2011. Changes in microbial community characteristics and soil organic matter with nitrogen additions in two tropical forests. *Ecology* 92 (3), 621–632.
- de Oliveira, T.B., de Lucas, R.C., Scarella, A.S. de A., Contato, A.G., Pasin, T.M., Martinez, C.A., Polizeli, M. de L.T. de M., 2020. Fungal communities differentially respond to warming and drought in tropical grassland soil. *Molecular Ecology* 29 (8), 1550–1559.
- de Vries, F.T., Griffiths, R.I., Bailey, M., Craig, H., Girlanda, M., Gweon, H.S., Hallin, S., Kaiser, A., Keith, A.M., Kretzschmar, M., Lemanceau, P., Lumini, E., Mason, K. E., Oliver, A., Ostle, N., Prosser, J.I., Thion, C., Thomson, B., Bardgett, R.D., 2018. Soil bacterial networks are less stable under drought than fungal networks. *Nature Communications* 9 (1), 3033.
- Dietterich, L.H., Bouskill, N.J., Brown, M., Castro, B., Chacon, S.S., Colburn, L., Cordeiro, A.L., García, E.H., Gordon, A.A., Gordon, E., Hedgpath, A., Konwent, W., Oppler, G., Reu, J., Tsiames, C., Valdes, E., Zeko, A., Cusack, D.F., 2022. Effects of experimental and seasonal drying on soil microbial biomass and nutrient cycling in four lowland tropical forests. *Biogeochemistry* 161, 227–250. <https://doi.org/10.1007/s10533-022-00980-2>.
- Doughty, C.E., Malhi, Y., Araujo-Murakami, A., Metcalfe, D.B., Silva-Espejo, J.E., Arroyo, L., Heredia, J.P., Pardo-Toledo, E., Mendizabal, L.M., Rojas-Landivar, V.D., Vega-Martinez, M., Flores-Valencia, M., Sibler-Rivero, R., Moreno-Vare, L., Viscarra, L.J., Chuviru-Castro, T., Osinaga-Becerra, M., Ledezma, R., 2014. Allocation trade-offs dominate the response of tropical forest growth to seasonal and interannual drought. *Ecology* 95 (8), 2192–2201.
- Easterling, D.R., Meehl, G.A., Parmesan, C., Changnon, S.A., Karl, T.R., Mearns, L.O., 2000. Climate extremes: observations, modeling, and impacts. *Science* 289 (5487), 2068–2074.
- Evans, S.E., Wallenstein, M.D., 2012. Soil microbial community response to drying and rewetting stress: does historical precipitation regime matter? *Biogeochemistry* 109 (1–3), 101–116.
- Evans, S.E., Wallenstein, M.D., 2014. Climate change alters ecological strategies of soil bacteria. *Ecology Letters* 17 (2), 155–164.
- Flemming, H.-C., Wingender, J., Szewzyk, U., Steinberg, P., Rice, S.A., Kjelleberg, S., 2016. Biofilms: an emergent form of bacterial life. *Nature Reviews Microbiology* 14 (9), 563–575.
- Foster, Z.S.L., Sharpton, T.J., Grünwald, N.J., 2017. Metacoder: an R package for visualization and manipulation of community taxonomic diversity data. *PLoS Computational Biology* 13 (2), e1005404.
- Freckman, D.W., 1986. The ecology of dehydration in soil organisms. In: *Membranes, Metabolism and Dry Organisms*. Cornell University Press, Ithaca, p. 16.
- Freitas, F., Alves, V.D., Torres, C.A.V., Cruz, M., Sousa, I., Melo, M.J., Ramos, A.M., Reis, M.A.M., 2011. Fucose-containing exopolysaccharide produced by the newly isolated Enterobacter strain A47 DSM 23139. *Carbohydrate Polymers* 83, 159–165. <https://doi.org/10.1016/j.carbpol.2010.07.034>.
- Frostegård, Å., Tunlid, A., Bååth, E., 2011. Use and misuse of PLFA measurements in soils. *Soil Biology and Biochemistry* 43, 1621–1625. <https://doi.org/10.1016/j.soilbio.2010.11.021>.
- Fukuyama, J., McMurdie, P.J., Dethlefsen, L., Relman, D.A., Holmes, S., 2012. Comparisons of distance methods for combining covariates and abundances in microbiome studies. *Pacific Symposium on Biocomputing*. Pacific Symposium on Biocomputing 213–224.
- Gatti, L.V., Gloor, M., Miller, J.B., Doughty, C.E., Malhi, Y., Domingues, L.G., Basso, L.S., Martinowski, A., Correia, C.S.C., Borges, V.F., Freitas, S., Braz, R., Anderson, L.O., Rocha, H., Grace, J., Phillips, O.L., Lloyd, J., 2014. Drought sensitivity of Amazonian carbon balance revealed by atmospheric measurements. *Nature* 506 (7486), 76–80.
- Hawkes, C.V., Keitt, T.H., 2015. Resilience vs. historical contingency in microbial responses to environmental change. *Ecology Letters* 18 (7), 612–625.
- He, D., Shen, W., Eberwein, J., Zhao, Q., Ren, L., Wu, Q.L., 2017. Diversity and co-occurrence network of soil fungi are more responsive than those of bacteria to shifts in precipitation seasonality in a subtropical forest. *Soil Biology and Biochemistry* 115, 499–510.
- Isobe, K., Allison, S.D., Khalili, B., Martiny, A.C., Martiny, J.B.H., 2019. Phylogenetic conservation of bacterial responses to soil nitrogen addition across continents. *Nature Communications* 10 (1), 2499.
- Isobe, K., Bouskill, N.J., Brodie, E.L., Suderth, E.A., Martiny, J.B.H., 2020. Phylogenetic conservation of soil bacterial responses to simulated global changes. *Philosophical Transactions of the Royal Society of London Series B Biological Sciences* 375, 20190242.
- Jackson, R.B., Lajtha, K., Crow, S.E., Hugelius, G., Kramer, M.G., Piñeiro, G., 2017. The ecology of soil carbon: pools, vulnerabilities, and biotic and abiotic controls. *Annual Review of Ecology Evolution and Systematics* 48 (Issue 1), 419–445. <https://doi.org/10.1146/annurev-ecolsys-112414-054234>.
- Jordan, S., Hutchings, M.J., Mascher, T., 2008. Cell envelope stress response in Gram-positive bacteria. *FEMS Microbiology Reviews* 32 (1), 107–146.
- Kielak, A.M., Castellane, T.C.L., Campanharo, J.C., Colnago, L.A., Costa, O.Y.A., Corradi da Silva, M.L., van Veen, J.A., Lemos, E.G.M., Kuramae, E.E., 2017. Characterization of novel Acidobacteria exopolysaccharides with potential industrial and ecological applications. *Scientific Reports* 7, 41193.
- Kuznetsova, A., Brockhoff, P.B., Christensen, R.H.B., 2017. lmerTest package: tests in linear mixed effects models. *Journal of Statistical Software* 82 (13), 1–26. <https://doi.org/10.18637/jss.v082.i13>, 10.18637/jss.v082.i13 (URL).
- Lajtha, K., Jarrell, W.M., 1999. *Soil Phosphorus. Standard Soil Methods For Long-Term Ecological Research*. Oxford University Press, New York, pp. 115–142.
- Lennon, J.T., den Hollander, F., Wilke-Berenguer, M., Blath, J., 2021. Principles of seed banks and the emergence of complexity from dormancy. *Nature Communications* 12 (1), 4807.
- Lenth, R., 2022. *emmeans: estimated marginal means, aka least-squares means*. R package version 1.8.1-1. <https://CRAN.R-project.org/package=emmeans>.
- Louca, S., Polz, M.F., Mazel, F., Albright, M.B.N., Huber, J.A., O'Connor, M.I., Ackermann, M., Hahn, A.S., Srivastava, D.S., Crowe, S.A., Doebeli, M., Parfrey, L.W., 2018. Function and functional redundancy in microbial systems. *Nature Ecology & Evolution* 2 (6), 936–943.
- Love, M.I., Huber, W., Anders, S., 2014. Moderated estimation of fold change and dispersion for RNA-seq data with DESeq2. *Genome Biology* 15 (12), 550.
- Malhi, Y., Grace, J., 2000. Tropical forests and atmospheric carbon dioxide. *Trends in Ecology & Evolution* 15 (8), 332–337. [https://doi.org/10.1016/s0169-5347\(00\)01906-6](https://doi.org/10.1016/s0169-5347(00)01906-6).
- Malik, A.A., Bouskill, N.J., 2022. Drought impacts on microbial trait distribution and feedback to soil carbon cycling. *Functional Ecology*. <https://doi.org/10.1111/1365-2435.14010>.
- Manzoni, S., Schaeffer, S.M., Katul, G., Porporato, A., Schimel, J.P., 2014. A theoretical analysis of microbial eco-physiological and diffusion limitations to carbon cycling in drying soils. *Soil Biology and Biochemistry* 73, 69–83.
- Manzoni, S., Schimel, J.P., Porporato, A., 2012. Responses of soil microbial communities to water stress: results from a meta-analysis. *Ecology* 93 (4), 930–938.
- Martiny, J.B.H., Jones, S.E., Lennon, J.T., Martiny, A.C., 2015. Microbiomes in light of traits: a phylogenetic perspective. *Science* 350 (6261), aac9323.
- Ma, X., Zhang, Q., Zheng, M., Gao, Y., Yuan, T., Hale, L., Van Nostrand, J.D., Zhou, J., Wan, S., Yang, Y., 2019. Microbial functional traits are sensitive indicators of mild disturbance by lamb grazing. *The ISME Journal* 13 (5), 1370–1373.
- Mayfield, C.I., Williams, S.T., Ruddick, S.M., Hatfield, H.L., 1972. Studies on the ecology of actinomycetes in soil IV. Observations on the form and growth of streptomycetes in soil. *Soil Biology and Biochemistry* 4 (1), 79–91.
- McMurdie, P.J., Holmes, S., 2013. *phyloseq: an R package for reproducible interactive analysis and graphics of microbiome census data*. *PLoS One* 8 (4), e61217.
- Meehl, G.A., Washington, W.M., Santer, B.D., Collins, W.D., Arblaster, J.M., Hu, A., Lawrence, D.M., Teng, H., Buja, L.E., Strand, W.G., 2006. Climate change projections for the twenty-first century and climate change commitment in the CCSM3. *Journal of Climate* 19 (Issue 11), 2597–2616. <https://doi.org/10.1175/jcli3746.1>.
- Mitchard, E.T.A., 2018. The tropical forest carbon cycle and climate change. *Nature* 559 (7715), 527–534.
- Nemergut, D.R., Cleveland, C.C., Wieder, W.R., Washenberger, C.L., Townsend, A.R., 2010. Plot-scale manipulations of organic matter inputs to soils correlate with shifts in microbial community composition in a lowland tropical rain forest. *Soil Biology and Biochemistry* 42 (12), 2153–2160.
- Nilsson, R.H., Larsson, K.-H., Taylor, A.F.S., Bengtsson-Palme, J., Jeppesen, T.S., Schigel, D., Kennedy, P., Picard, K., Glöckner, F.O., Tedersoo, L., Saar, I., Köljalg, U., Abarenkov, K., 2019. The UNITE database for molecular identification of fungi: handling dark taxa and parallel taxonomic classifications. *Nucleic Acids Research* 47 (D1), D259–D264.
- Nottingham, A.T., Meir, P., Velasquez, E., Turner, B.L., 2020. Soil carbon loss by experimental warming in a tropical forest. *Nature* 584 (7820), 234–237.
- O'Connell, C.S., Ruan, L., Silver, W.L., 2018. Drought drives rapid shifts in tropical rainforest soil biogeochemistry and greenhouse gas emissions. *Nature Communications* 9 (1), 1348.
- Oksanen, J., Others, 2011. Multivariate analysis of ecological communities in R: vegan tutorial. R Package Version 1 (7), 1–43.
- Oren, A., 1999. Bioenergetic aspects of halophilism. *Microbiology and Molecular Biology Reviews: Microbiology and Molecular Biology Reviews* 63 (2), 334–348.
- Parada, A.E., Needham, D.M., Fuhrman, J.A., 2016. Every base matters: assessing small subunit rRNA primers for marine microbiomes with mock communities, time series and global field samples. *Environmental Microbiology* 18 (5), 1403–1414. <https://doi.org/10.1111/1462-2920.13023>.

- Pavoine, S., Dufour, A.-B.A.-B., Chessel, D., 2004. From dissimilarities among species to dissimilarities among communities: a double principal coordinate analysis. *Journal of Theoretical Biology* 228 (4), 523–537.
- Phillips, O.L., Aragão, L.E.O.C., Lewis, S.L., Fisher, J.B., Lloyd, J., López-González, G., Malhi, Y., Monteagudo, A., Peacock, J., Quesada, C.A., van der Heijden, G., Almeida, S., Amaral, I., Arroyo, L., Aymard, G., Baker, T.R., Bánki, O., Blanc, L., Bonal, D., et al., 2009. Drought sensitivity of the Amazon rainforest. *Science* 323 (5919), 1344–1347.
- Purdom, E., 2011. Analysis of a data matrix and a graph: metagenomic data and the phylogenetic tree. *Annals of Applied Statistics* 5 (4), 2326–2358.
- Pyke, C.R., Condit, R., Aguilar, S., Lao, S., 2001. Floristic composition across a climatic gradient in a neotropical lowland forest. *Journal of Vegetation Science: Official Organ of the International Association for Vegetation Science* 12 (4), 553–566.
- Quast, C., Pruesse, E., Yilmaz, P., Gerken, J., Schweer, T., Yarza, P., Peplies, J., Glockner, F.O., 2013. The SILVA ribosomal RNA gene database project: improved data processing and web-based tools. *Nucleic Acids Research* 41 (Database issue), D590–D596.
- Quince, C., Lanzen, A., Davenport, R.J., Turnbaugh, P.J., 2011. Removing noise from pyrosequenced amplicons. *BMC Bioinformatics* 12, 38. <https://doi.org/10.1186/1471-2105-12-38>.
- Rocca, J.D., Simonin, M., Blaszcak, J.R., Ernakovich, J.G., Gibbons, S.M., Midani, F.S., Washburne, A.D., 2018. The microbiome stress project: toward a global meta-analysis of environmental stressors and their effects on microbial communities. *Frontiers in Microbiology* 9, 3272.
- Römling, U., Galperin, M.Y., 2015. Bacterial cellulose biosynthesis: diversity of operons, subunits, products, and functions. *Trends in Microbiology* 23 (9), 545–557.
- Ross, P., Mayer, R., Benziman, M., 1991. Cellulose biosynthesis and function in bacteria. *Microbiological Reviews* 55, 35–58. <https://doi.org/10.1128/mr.55.1.35-58.1991>.
- Schimel, J.P., 2018. Life in dry soils: effects of drought on soil microbial communities and processes. *Annual Review of Ecology Evolution and Systematics* 49 (Issue 1), 409–432. <https://doi.org/10.1146/annurev-ecolsys-110617-062614>.
- Schliep, K.P., 2011. phangorn: phylogenetic analysis in R. *Bioinformatics* 27 (4), 592–593.
- Shade, A., Peter, H., Allison, S.D., Bahn, D.L., Berga, M., Bürgmann, H., Huber, D.H., Langenheder, S., Lennon, J.T., Martiny, J.B.H., Matulich, K.L., Schmidt, T.M., Handelsman, J., 2012. Fundamentals of microbial community resistance and resilience. *Frontiers in Microbiology* 3, 417.
- Six, J., 2012. Fungal friends against drought. *Nature Climate Change* 2 (4), 234–235.
- Stewart, R.H., Stewart, J.L., Others, 1980. Geologic map of the Panama canal and vicinity, republic of Panama. <https://pubs.er.usgs.gov/publication/11232>.
- Sullivan, M.J.P., Lewis, S.L., Affum-Baffoe, K., Castilho, C., Costa, F., Sanchez, A.C., Ewango, C.E.N., Hubau, W., Marimon, B., Monteagudo-Mendoza, A., Qie, L., Sonké, B., Martinez, R.V., Baker, T.R., Brienen, R.J.W., Feldpausch, T.R., Galbraith, D., Gloor, M., Malhi, Y., et al., 2020. Long-term thermal sensitivity of Earth's tropical forests. *Science* 368 (6493), 869–874.
- Supramaniam, Y., Chong, C.-W., Silvaraj, S., Tan, I.K.-P., 2016. Effect of short term variation in temperature and water content on the bacterial community in a tropical soil. *Applied Soil Ecology: A Section of Agriculture, Ecosystems & Environment* 107, 279–289.
- Team, R., 2016. RStudio. Integrated development environment for R., Boston, MA.
- Tecon, R., Ebrahimi, A., Kleyer, H., Erev Levi, S., Or, D., 2018. Cell-to-cell bacterial interactions promoted by drier conditions on soil surfaces. *Proceedings of the National Academy of Sciences of the United States of America* 115 (39), 9791–9796.
- Turner, B.L., Engelbrecht, B.M.J., 2011. Soil organic phosphorus in lowland tropical rain forests. *Biogeochemistry* 103 (1–3), 297–315.
- Ude, S., Arnold, D.L., Moon, C.D., Timms-Wilson, T., Spiers, A.J., 2006. Biofilm formation and cellulose expression among diverse environmental *Pseudomonas* isolates. *Environmental Microbiology* 8, 1997–2011. <https://doi.org/10.1111/j.1462-2920.2006.01080.x>.
- Uhlirová, E., Elhottová, D., Tríška, J., Santrúcková, H., 2005. Physiology and microbial community structure in soil at extreme water content. *Folia Microbiologica* 50 (2), 161–166.
- Veach, A.M., Chen, H., Yang, Z.K., Labbe, A.D., Engle, N.L., Tschaplinski, T.J., Schadt, C. W., Cregger, M.A., 2020. Plant hosts modify belowground microbial community response to extreme drought. *mSystems* 5 (3). <https://doi.org/10.1128/mSystems.00092-20>.
- Ward, C.S., Yung, C.-M., Davis, K.M., Blinebry, S.K., Williams, T.C., Johnson, Z.I., Hunt, D.E., 2017. Annual community patterns are driven by seasonal switching between closely related marine bacteria. *The ISME Journal* 11 (11), 2637.
- Ward, N.L., Challacombe, J.F., Janssen, P.H., Henrissat, B., Coutinho, P.M., Wu, M., Xie, G., Haft, D.H., Sait, M., Badger, J., Barabote, R.D., Bradley, B., Brettin, T.S., Brinkac, L.M., Bruce, D., Creasy, T., Daugherty, S.C., Davidsen, T.M., DeBoy, R.T., et al., 2009. Three genomes from the phylum acidobacteria provide insight into the lifestyles of these microorganisms in soils. *Applied and Environmental Microbiology* 75 (7), 2046–2056.
- Weatherburn, M.W., 1967. Phenol-hypochlorite reaction for determination of ammonia. *Analytical Chemistry* 39 (8), 971–974. <https://doi.org/10.1021/ac60252a045>.
- Williams, M.A., Rice, C.W., 2007. Seven years of enhanced water availability influences the physiological, structural, and functional attributes of a soil microbial community. *Applied Soil Ecology* 35 (3), 535–545. <https://doi.org/10.1016/j.apsoil.2006.09.014>.
- Wolf, A.B., Vos, M., de Boer, W., Kowalchuk, G.A., 2013. Impact of matric potential and pore size distribution on growth dynamics of filamentous and non-filamentous soil bacteria. *PLoS One* 8 (12), e83661.
- Wright, E.S., 2015. DECIPIERRE harnessing local sequence context to improve protein multiple sequence alignment. *BMC Bioinformatics* 16, 322.
- Zhang, J., Liu, S., Liu, C., Wang, H., Luan, J., Liu, X., Guo, X., Niu, B., 2021. Different mechanisms underlying divergent responses of autotrophic and heterotrophic respiration to long-term throughfall reduction in a warm-temperate oak forest.
- Zhao, Q., Shen, W., Chen, Q., Helmisaari, H.-S., Sun, Q., Jian, S., 2018. Spring drying and intensified summer rainfall affected soil microbial community composition but not enzyme activity in a subtropical forest. *Applied Soil Ecology: A Section of Agriculture, Ecosystems & Environment* 130, 219–225.
- Zhou, L., Liu, Y., Zhang, Y., Sha, L., Song, Q., Zhou, W., Balasubramanian, D., Palingamoorthy, G., Gao, J., Lin, Y., Li, J., Zhou, R., Zar Myo, S.T., Tang, X., Zhang, J., Zhang, P., Wang, S., Grace, J., 2019. Soil respiration after six years of continuous drought stress in the tropical rainforest in Southwest China. *Soil Biology and Biochemistry* 138, 107564.